

# Multiple Structures of (110) CSL Twist Boundaries in fcc Metals

Abdul GHAFOOR, Barkat Ali Shafiq FARIDI, Aftab AHMAD

*Department of Physic, Islamia University,  
Bahawalpur-PAKISTAN*

Received 12.10.1998

## Abstract

The geometry of different possible structures of (110) fcc twist boundaries is explored. Computer simulation of all possible low energy structures have been carried out for  $\Sigma = 3$  and  $\Sigma = 9$  twist boundaries using many-body potentials representing copper, silver and gold. Low symmetry structures are found to have lower energies than the high symmetry CSL structures.

## 1. Introduction

Most engineering applications of the materials involve their use in polycrystalline form. It is therefore important to have an understanding of the structure and properties of the interfaces between grains forming such materials. Most common structures of grain boundaries are classified as twin-, tilt- and twist-boundaries. Tilt boundaries are those in which two grains are related by a rotation about an axis lying in the grain boundary. Twist boundaries have their axis of rotation perpendicular to the grain boundary. In these, two grains meeting at a grain boundary have atoms located at the points of two lattices related by a rotation. If these lattices are considered to interpenetrate and fill all space none of the points will in general coincide. However a single point from each lattice may be brought into coincidence by translation, an infinite number of points may coincide. These points then form a one-, two and three-dimensional array which is known as a coincidence site lattice (CSL). The reciprocal density of coincident sites relative to the original lattice is denoted by  $\Sigma$ .

Computer simulation techniques have recently been used to determine the structure and energy of coincident site lattice CSL (111) and (001) twist boundaries [1,2]. Bristowe and Crocker [3] found three distinct stable structures of (001) twist boundary, here two of which involved relative translations of the grains parallel to the boundary and away from the reference CSL configurations. Later Ingle and Crocker [4] studied (110) twist

boundaries and found that three stable structures exist which involve relative translations of the two grains parallel to the interface. In each case [3,4] the structures have nearly equal energies, so in practice two or more types for single twist boundary may occur in real crystals. This implies that complex networks of grain boundary dislocations are likely to exist.

Computer simulation studies of structures of other types of interface in metals [5,6] have shown that in many cases only one low energy structure arises and that may have low symmetry as well. Thus, it is not even clear at this time whether in poly-crystals, symmetrical or asymmetrical grain boundary plane orientation prevails, or even, whether symmetrical configurations are energetically favoured over asymmetrical ones. However, experimental evidences [7,8] suggest that asymmetrical grain boundaries are not as uncommon as sometimes where thought, particularly within the framework of the geometrical grain boundary models [9, 10].

The most crucial decision for the simulation of a specific type of defects is the choice of an appropriate interatomic potential. The energy of the planar defects, such as grain boundaries, is almost completely controlled by the strong repulsion between the boundary atoms, which are at distances shorter than those in the perfect crystal. The CSL twist boundary structures in copper have been simulated employing Embedded Atom Method and Lennard-Jones two-body potentials [11,12]. Unfortunately both the potentials give zero energy for  $\Sigma = 3$  (111) twist boundary. In this boundary one in three of the atoms are located at coincident sites of the two grains. Many-body potentials developed by Ackland et al. for fcc metals [13] have overcome this deficiency and give energy for (111) twist boundary within the experimentally measured values [1]. According to this potential energy (of an atom labeled  $i$ ) is written as:

$$U_i = 1/2 \sum_j V(r_{ij}) - \left[ \sum_j \phi(r_{ij}) \right]^{1/2}$$

The summation extends to all atoms of the system. Their pair potential function  $V$  and embedded cohesive potential  $\phi$  are:

$$V(r) = \sum_{k=1}^6 a_k (r_k - r)^3 H(r_k - r)$$

and

$$\phi(r) = \sum_{k=1}^2 A_k (R_k - r)^3 H(R_k - r),$$

where

$$H(x) = \begin{cases} 1 & \text{for } x > 0 \\ 0 & \text{for } x \leq 0. \end{cases}$$

Cut-off radii  $r_1$  and  $R_1$  are taken equal to the third neighbour spacing. The coefficients  $a_k$  and  $A_k$  have been determined by fitting exactly to the equilibrium fcc lattice parameter

$\mathbf{a}$ , the cohesive energy  $E_c$ , the elastic constants  $C_{11}$ ,  $C_{12}$  and  $C_{44}$ , the relaxed vacancy formation energy  $E_f^v$  and the stacking fault energy  $\gamma$ . The fitted coefficients of  $V$  and  $\phi$  for copper are summarized in Table 1.

**Table 1.** Fitted coefficients by Ackland et al. [13] for  $V$  and  $\phi$

Coefficient	Value (eV)	Coefficient	Value ( $\mathbf{a}$ )
$a_1$	29.059214	$r_1$	1.2247449
$a_2$	-140.056810	$r_2$	1.1547054
$a_3$	130.073310	$r_3$	1.1180065
$a_4$	-17.481350	$r_4$	1.0000000
$a_5$	31.825460	$r_5$	0.8660254
$a_6$	71.587490	$r_6$	0.7071068
$A_1$	9.806694	$R_1$	1.2247449
$A_2$	16.774638	$R_2$	1.1180065

As these potentials have successfully been used for the simulation of (111) and (001) twist boundaries [1,2] in fcc metals, here these have been employed to simulate  $\Sigma = 3$  and  $\Sigma = 9$  (110) twist boundaries in copper, silver and gold. The simulation methods adopted and results obtained are given in section 2. The significance of the results is discussed in the last section.

## 2. Computational Methods and Results

Rectangular prism shape model crystallite was generated with orthogonal axes for the simulation of twist boundaries. The atoms in the active computational region were completely free to move under the applied potential. This region was surrounded by a mantle reasonably thick such that the atoms of the computational cell have full quota of their neighbors. The mantle atoms on the faces parallel to the twist boundary were kept fixed and those on the rest of the faces were moveable due to periodic boundary conditions. This procedure effectively simulates an infinite boundary. The twist boundaries under study were generated in the middle of the model so as to keep them at equal distances from the fixed boundaries. Minimum shuffle magnitudes required for the generation of twisted model, were determined from the geometrical sketches of the perfect model. This procedure has the advantage that the original rectangular prism shape of the model remains unchanged even after twisting half of the crystal. The other possible structures of each of the boundaries could be obtained by displacing two grains with respect to each other. Three special cases of particular interest arise corresponding to the displacement of  $\mathbf{d}_1/2$ ,  $\mathbf{d}_2/2$  and  $(\mathbf{d}_1 + \mathbf{d}_2)/2$ , where  $\mathbf{d}_1$  &  $\mathbf{d}_2$  represent the complete pattern shift of the boundary.

In order to minimise energy of the model, the method of conjugate gradients [14] was adopted in FORTRAN codes. The method of conjugate gradients moves downhill in an N-dimensional space, in directions which are orthogonal to each other. For a particular

search direction  $\mathbf{s}$ , the gradient  $\mathbf{g}$  satisfies the condition

$$\mathbf{g} \cdot \mathbf{s} = 0.$$

After each new choice of direction  $\mathbf{s}$ , an appropriate step length in that direction is chosen. It is often found that after a certain number of iterations, a greater decrease in energy can be obtained by returning to the steepest descent rather than continuing in yet another conjugate direction

Computational models were allowed to relax after generating the required twist so that each atom could move to its minimum energy position under the applied potential. Static simulation has been carried out, and the equilibrium configuration corresponds to atoms at rest, such that the calculations are at 0 K.

### 2.1. The $\Sigma = 3$ Twist Boundary

In order to simulate  $\Sigma = 3$  (110) twist boundary, the model crystallite generated was bounded by  $(\bar{1}11)$ ,  $(\bar{1}1\bar{2})$  and (110) face. Fixed boundary conditions were imposed on (110) faces while  $(\bar{1}11)$  and  $(\bar{1}1\bar{2})$  faces were simulated under cyclic boundary conditions. The active computational cell comprised of 5 $(\bar{1}11)$ , 12 $(\bar{1}1\bar{2})$  and 60(110) planes. The CSL twist boundary (referred to as type **A**) was generated in the middle of the model in [110] direction by applying atomic shuffle technique to the non-CSL atoms of the upper half of the crystallite. Other three possible structures of types **B**, **C** and **D** were obtained by moving the upper grain by the magnitudes  $1/6[\bar{1}11]\mathbf{a}$ ,  $1/12[\bar{1}1\bar{2}]\mathbf{a}$  and  $1/4[\bar{1}10]\mathbf{a}$ , respectively.

Minimum energy configurations of all four types were obtained by relaxing the computer models, using the conjugate gradient method. Studying the resulting structures, two distinct type of displacements were noted to occur, one for CSL and other for non-CSL atoms. As in the case of (111) twist boundaries [1], the displacements for all CSL sites were normal to the boundary plane, while non-CSL sites had components both parallel and normal to it. Of course, equal and opposite displacements arose for equivalent sites on both sides of the interface. Only significant displacements were observed around the boundary. The volume increases that occurred at interfaces were accommodated by compressive strains in the model as a whole. To eliminate these strains, simulations were carried out in which the two grains were deliberately moved apart and then the models were allowed to relax. Stable structures were found for all four types of the boundary. The energies obtained along with the volume expansions normal to the interface are summarized in Table 2 while relaxed structure for  $\Sigma = 3$  type **A** boundary is shown in Fig. 1.

### 2.2. The $\Sigma = 9$ Twist Boundary

To study  $\Sigma = 9$ (110) twist boundary structures, a rectangular crystallite of atoms comprising of 18 $(\bar{2}21)$ , 18 $(\bar{4}1\bar{4})$  and 60(110) planes was generated. Appropriate number of mantle atomic planes were added on all sites of the computational model and periodic boundary conditions were imposed on  $(\bar{2}21)$  and  $(\bar{4}1\bar{4})$  faces. The atoms of the mantle region on the faces parallel to the boundary were treated as fixed. The  $\Sigma = 9$  CSL

boundary (type **A**) was generated in the middle of the model in  $[110]$  direction by the minimum shuffle of non-CSL atoms of one half of the crystallite. The remaining three structures of types **B**, **C** and **D** were obtained from type **A** structure, by translating the upper half grain parallel to the boundary plane through magnitudes  $1/18[\bar{2}21]\mathbf{a}$ ,  $1/36[\bar{1}1\bar{4}]\mathbf{a}$  and  $1/36[\bar{5}5\bar{2}]\mathbf{a}$ , respectively.

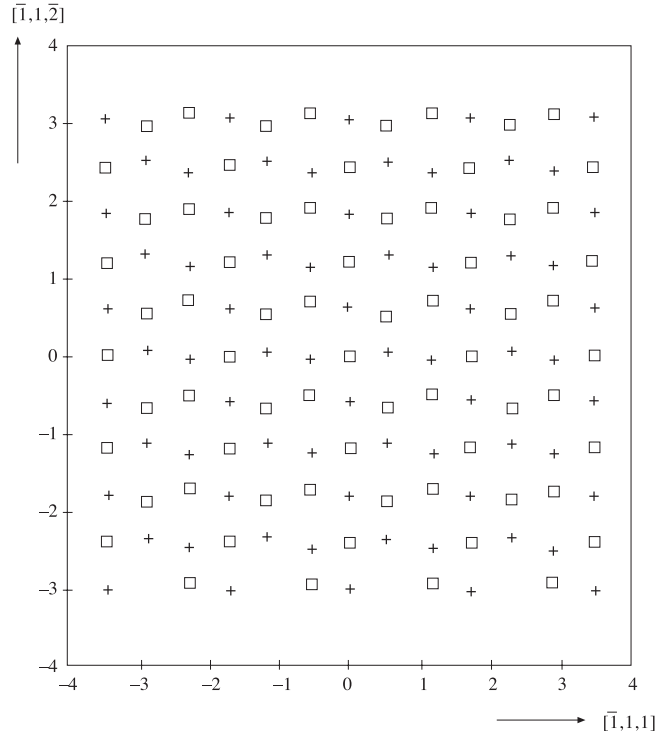


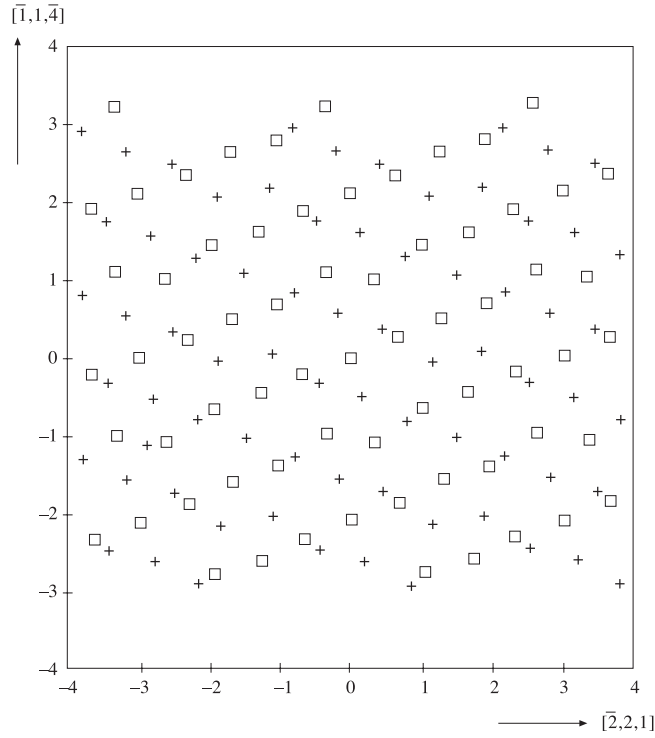
**Figure 1.** A relaxed structure of  $\Sigma = 3$  type **A** twist boundary projected on the  $(110)$  plane. The atoms of the planes immediately above and below the boundary are represented by  $\square$  and  $+$ .

The long-range compressive strains in the models were eliminated by allowing volume increases. During relaxation, as in the case of  $\Sigma = 3$  boundary, the displacement for CSL sites were observed to be normal to the boundary only, while non-CSL sites had both normal and parallel components. The displacements were significant only near boundary. All four relaxed structures of  $\Sigma = 9$  twist boundary were found to be stable. The energies for types **A**, **B**, **C** and **D** boundaries in copper were 1371, 1305, 1405 and 1402 mJ/m<sup>2</sup> and volume expansions  $10, 6, 30$  &  $16 \times 10^{-3} \mathbf{a}$ , respectively. The results for boundaries in silver and gold are included in Table 2 along with earlier results of copper [4] for comparison. The relaxed structure of the CSL (type **A** twist boundary in copper in shown in Fig. 2.

**Table 2.** Twist boundary energies for fcc metals, in units of  $\text{mJ}/\text{m}^2$ , translation and volume expansion in units of lattice parameter  $\mathbf{a}$ .

Type	Translation	Energy ( $\text{mJ}/\text{m}^2$ ) / Expansion ( $\mathbf{a}$ )			
		Copper*	Copper	Silver	Gold
$\Sigma = 3$ A	— — —	1398 /0.014	1433 /0.086	1099 /0.130	1081 /0.101
B	$1/6[\bar{1}11]$	1363 /0.032	1272 /0.104	975 /0.124	915 /0.118
C	$1/12[\bar{1}1\bar{2}]$	1475 /0.056	1389 /0.126	1009 /0.148	1019 /0.145
D	$1/4[\bar{1}10]$	1677 /0.047	1511 /0.106	1065 /0.154	1030 /0.152
$\Sigma = 9$ A	— — —	1410 /0.010	1371 /0.116	1046 /0.126	1009 /0.140
B	$1/18[\bar{2}21]$	1403 /0.006	1305 /0.128	973 /0.154	912 /0.132
C	$1/36[\bar{1}1\bar{4}]$	1466 /0.030	1405 /0.112	1024 /0.140	986 /0.138
D	$1/35[\bar{5}5\bar{5}]$	1489 /0.016	1402 /0.116	1030 /0.130	986 /0.133

\*The values in this column are taken from Ingle and Crocker [4].

**Figure 2.** A relaxed structure of  $\Sigma = 9$  type A twist boundary projected on the (001) plane.

### 3. Discussion

The atomic structures of (110) twist boundaries have been investigated with misori-

entation angles of  $70.5^\circ$  and  $38.9^\circ$ . The results obtained are very different from those of earlier work on (111) and (100) twist boundaries [1,2]. In particular the lowest energy structures for both the  $\Sigma = 3$  and  $\Sigma = 9$  boundaries have lower symmetry than the CSL. Nonetheless the high symmetry CSL structures provide a useful starting point for investigation.

Ingle and Crocker [4] have used copper pair potential [15] for similar calculations of (110) twist boundaries and their results for copper are included in Table 2- for comparison. In the present work, energies of all four types of twist boundaries are lower than their corresponding values with only one exception of  $\Sigma = 3$  type **A** boundary, where present energy is slightly higher. Theoretical or experimental results for these boundaries in silver and gold are not available in literature and therefore could not be compared. In general, twist boundary energies for copper are higher than silver and those of silver are higher than gold. There is also one exemption to be noted from the result summary of Table 2 which is for  $\Sigma = 3$  type **C** silver energy being 0.1% lower than that of the same boundary in gold.

It is observed that type **B** structures for both of the twist boundaries in copper, silver and gold, have the lowest energy among all four possible structures considered. For silver and gold, type **A** boundary has the highest energies for both the twist boundaries. However, copper type **D** boundary structure has the highest energy.

Although the computing procedure was capable of accommodating rigid-body translations, both parallel and perpendicular to the twist boundaries, additional rigid rotations, increasing or decreasing the angle of twist from the exact CSL values could not be introduced in the present models. However, during relaxation long-range torsion of model was not observed in the present investigations.

### Acknowledgement

Financial support from NSRD Board is gratefully acknowledged.

### References

- [1] A Ghafoor, S. A. Ahmad and B. A. S. Faridi, *J. Nat Sci. Maths.*, **36** (1996) 33.
- [2] A. Ghafoor, S. A. Ahmad and B. A. S. Faridi, *Tr. J. of Phys.*, **22** (1998) 789.
- [3] P. D. Bristowe and A. G. Crocker, *Phil. Mag.*, **38** (1978) 487.
- [4] K. W. Ingle and A. G. Crocker, *Phil. Mag.*, **41** (1980) 713.
- [5] B. A. S. Faridi, S. A. Ahmad and M. A. Choudhry, *Indian J. of Pure & Appl. Phys.*, **29** (1991) 796.
- [6] A. G. Crocker and B. A. Faridi, *Acta Metall.*, **28** (1980) 549.
- [7] C. B. Carter, *Acta Metall.*, **36** (1988) 2753.
- [8] K. L. Merkle, J. F. Reddy and C. L. Wiley, *Ultramicroscopy*, **18** (1985) 281.

- [9] D. G. Brandon, B. Ralph, S. Ranganathan and M. S. Wald, *Acta Metall.*, **12** (1964) 318.
- [10] W. Bollman, *Crystal Defects and Crystalline Interfaces*, (Springer, Berlin 1970).
- [11] D. Wolf, *Acta Metall.*, **38** (1990) 791.
- [12] D. Wolf, *Acta Metall.*, **37** (1989) 1983.
- [13] G. J. Ackland, G. Tichy, V. Vitek, M. W. Finnis, *Phil. Mag.*, **56** (1987) 735.
- [14] R. Fletcher and C. M. Reeves, *Comput. J.* **7** (1964) 149.
- [15] A. G. Crocker, M. Doneghan and K. W. Ingle, *Phil. Mag.* **41** (1980) 21.